

The Highly Damped Quasinormal Modes of d -dimensional Reissner-Nordström Black Holes in the Small Charge Limit

Ramin G. Daghigh, Gabor Kunstatter, Dave Ostapchuk, and Vince Bagnulo

*Physics Department, University of Winnipeg, Winnipeg, Manitoba, Canada R3B 2E9
and*

Winnipeg Institute for Theoretical Physics, Winnipeg, Manitoba

Abstract

We analyze in detail the highly damped quasinormal modes of d -dimensional Reissner-Nordström black holes with small charge, paying particular attention to the large but finite damping limit in which the Schwarzschild results should be valid. In the infinite damping limit, we confirm using different methods the results obtained previously in the literature for higher dimensional Reissner-Nordström black holes. Using a combination of analytic and numerical techniques we also calculate the transition of the real part of the quasinormal mode frequency from the Reissner-Nordström value for very large damping to the Schwarzschild value of $\ln(3)T_{bh}$ for intermediate damping. The real frequency does not interpolate smoothly between the two values. Instead there is a critical value of the damping at which the topology of the Stokes/anti-Stokes lines change, and the real part of the quasinormal mode frequency dips to zero.

1. Introduction

There exist by now many calculations of the highly damped quasinormal modes (QNMs) of a large variety of black holes. Since the highly damped modes are not directly observable, these calculations are mainly motivated by the proposal, originating with Hod[1] and more recently propounded by Dreyer[2] in the context of loop quantum gravity, that these modes may be providing information about the semi-classical quantum spectrum of black holes. This proposal was prompted in part by the apparent universality of the real part of the frequency in the highly damped limit, as well as by its special numerical value for Schwarzschild black holes, namely:

$$\omega_R \xrightarrow{|\omega_I| \rightarrow \infty} \ln(3)T_{bh}/\hbar, \quad (1.1)$$

where T_{bh} is the Hawking temperature of the black hole. The frequency and the damping are proportional to the temperature on dimensional grounds for single horizon black holes, but the coefficient $\ln(3)$ allows, on application of the Bohr correspondence principle, an elegant statistical interpretation[1, 3] of the resulting Bekenstein-Hawking entropy spectrum. We refer the reader to the literature for details[4]. Although this special value has been shown to be valid for a large class of single horizon black holes[5, 6, 7, 8] this simple relationship between frequency and temperature breaks down for multi-horizon black holes.

It was shown first by Motl and Neitzke[5] and then confirmed by Andersson and Howls[9] that for Reissner-Nordström (R-N) black holes the real part of the highly damped QNM frequency in four dimension approaches $\ln(5)T_{bh}$ as the charge goes to zero. The general validity of this result was verified by Natario and Schiappa[10], who calculated the R-N highly damped spectrum in arbitrary spacetime dimensions. The apparent contradiction between the zero charge limit of the R-N case, and the Schwarzschild value was explained heuristically by the authors of [9]. They noted, that, while the $\ln(5)$ represented the correct R-N result for very high damping, one expects an intermediate range of damping for which the Schwarzschild value of the real frequency is correct. Order of magnitude arguments suggest this range in $4-d$ to be:

$$1 \ll |\omega|^2 M^2 \ll M^8/q^8 \quad (1.2)$$

The purpose of the present paper is two-fold. First, we calculate the highly damped QNMs of d -dimensional R-N black holes with the small charge using the techniques of Andersson and Howls[9], thereby confirming the results of Natario and Schiappa[10], who used the monodromy method of Ref.[5, 11]. Secondly, and more significantly, we use a combination of analytic and numerical techniques to analyze the limit of large but finite damping where the Schwarzschild limit is approached. For four and five spacetime dimension R-N black holes we explicitly calculate the spectrum in the transition region from $\ln(3 + 4 \cos(\frac{d-3}{2d-5}\pi))T_{bh}$ for very large damping to the Schwarzschild value of $\ln(3)T_{bh}$. The real frequency does not interpolate smoothly between the two values. Instead there is generically a critical value of the damping at which the Stoke/anti-Stokes lines change topology and the real part of the frequency dips to zero. This behaviour seems to be the analogue of the algebraically special frequencies (for a recent discussion see Berti[12]) that mark the onset of the high damping regime. We provide general arguments that suggest the persistence of this behaviour for all spacetime dimensions.

The paper is organized as follows. In Section 2 we describe the general formalism. Section 3 summarizes the results of the calculation in the large damping limit for metric perturbations (tensor, vector, and scalar) of Schwarzschild and R-N. The former reviews well known results while the latter provides independent confirmation of [10]. Section 4 presents the details of the calculation for axial perturbations in the intermediate region in four dimensions, while Section 5 does the same for five dimensions. (Tensor and scalar perturbations cannot be done using our numerical techniques, because a crucial term in the effective potential vanishes precisely in that limit.) The final section describes general arguments for the persistence of the qualitative features of our results in higher dimensions, and closes with some conclusions.

2. General Formalism

It was shown by Ishibashi and Kodama in [13], [14], and [15] that various classes of non-rotating black hole metric perturbations in a spacetime with dimension $d > 3$ are governed generically by a Schrödinger wave-like equation of the form:

$$\frac{d^2\psi}{dz^2} + [\omega^2 - V(r)]\psi = 0, \quad (2.1)$$

for perturbations that depend on time as $e^{-i\omega t}$. The Tortoise coordinate z is defined by

$$dz = \frac{dr}{f(r)}, \quad (2.2)$$

where $f(r)$ is related to the spacetime geometry, and is given by

$$f(r) = 1 - \frac{2\mu}{r^{d-3}} + \frac{\theta^2}{r^{2d-6}} - \lambda r^2. \quad (2.3)$$

The ADM mass, M , of the black hole is related to the parameter μ by

$$M = \frac{(d-2)A_{d-2}}{8\pi G_d}\mu, \quad (2.4)$$

where A_n is the area of a unit n -sphere,

$$A_n = \frac{2\pi^{\frac{n+1}{2}}}{\Gamma\left(\frac{n+1}{2}\right)}. \quad (2.5)$$

The electric charge, q , of the black hole is,

$$q^2 = \frac{(d-2)(d-3)}{8\pi G_d}\theta^2, \quad (2.6)$$

while the value of the cosmological constant, Λ , is given by

$$\Lambda = \frac{(d-1)(d-2)}{2}\lambda. \quad (2.7)$$

In this paper we only deal with asymptotically flat black holes where $\lambda = \Lambda = 0$. The units we will be using are $c = G_d = \hbar = 1$.

The effective potential $V(r)$, was found explicitly by Ishibashi and Kodama[13, 14, 15] for scalar (reducing to polar at $d = 4$), vector (reducing to axial at $d = 4$), and tensor (non-existing at $d = 4$) perturbations. The effective potential for tensor perturbations has been shown [16, 17] to be equivalent to that of the decay of test scalar field in a black hole background. The effective potential is zero at both the horizon ($z \rightarrow -\infty$) and spatial infinity ($z \rightarrow \infty$). In the case of QNMs, the asymptotic behavior of the solutions is chosen to be

$$\psi(z) \approx \begin{cases} e^{-i\omega z} & \text{as } z \rightarrow -\infty \text{ (} x \rightarrow x_h \text{)} , \\ e^{+i\omega z} & \text{as } z \rightarrow \infty \text{ (} x \rightarrow \infty \text{)} , \end{cases} \quad (2.8)$$

which represents an outgoing wave at infinity and an ingoing wave at the horizon. Since the tortoise coordinate is multi-valued, it is more convenient to work in the complex r -plane. After rescaling the wavefunction $\psi = \Psi/\sqrt{f}$ we obtain

$$\frac{d^2\Psi}{dr^2} + R(r)\Psi = 0 , \quad (2.9)$$

where

$$R(r) = \frac{\omega^2}{f^2(r)} - U(r) , \quad (2.10)$$

with

$$U(r) = \frac{V(r)}{f^2} + \frac{1}{2} \frac{f''}{f} - \frac{1}{4} \left(\frac{f'}{f} \right)^2 . \quad (2.11)$$

Here prime denotes differentiation with respect to r .

3. Large Damping Limit and Universality

We now consider the QNMs in the infinite damping limit where

$$|\omega^2| \rightarrow [\text{Im } \omega]^2 \rightarrow \infty . \quad (3.1)$$

Since we will be using complex analytic techniques, in principle the behaviour of $U(r)$ on the entire complex plane may be relevant. However, in the infinite limit case, the ω^2/f^2 term in $R(r)$ will dominate $U(r)$ everywhere, unless one of the terms in $U(r)$ diverges. This can only happen at the origin, or at the horizon. However, since ω^2/f^2 also diverges at the horizon, it will dominate there as well in the large damping limit. Thus, only the dominant term of $U(r)$ near the origin is relevant in this limit and $R(r)$ can be approximated on the entire complex plane by

$$R(r) \sim \frac{\omega^2}{f^2} - \frac{J^2 - 1}{4r^2} , \quad (3.2)$$

where J is determined by the type of metric perturbation. In particular, for different

perturbations we find:

$$J^2 - 1 = \begin{cases} -1 & \text{Tensor Perturbation } (\theta = 0 \text{ and } n > 2) , \\ n(n-2) & \text{Tensor Perturbation } (\theta \neq 0 \text{ and } n > 2) , \\ 4n^2 - 1 & \text{Vector Perturbation } (\theta = 0) , \\ 3n(3n-2) & \text{Vector Perturbation } (\theta \neq 0) , \\ -1 & \text{Scalar Perturbation } (\theta = 0) , \\ n(n-2) & \text{Scalar Perturbations } (\theta \neq 0) , \end{cases} \quad (3.3)$$

where $n = d - 2$. The universality of the infinite damping QNM frequency can, to a large extent, be attributed to the simple form of (3.2) in this limit.

In the WKB analysis, the two solutions to Eq. (2.9) are approximated by

$$\begin{cases} \Psi_1^{(t)}(x) = Q^{-1/2}(x) \exp [+i \int_t^x Q(x') dx'] , \\ \Psi_2^{(t)}(x) = Q^{-1/2}(x) \exp [-i \int_t^x Q(x') dx'] , \end{cases} \quad (3.4)$$

where

$$Q^2(r) = R(r) - \frac{1}{4r^2} \sim \frac{\omega^2}{f^2} - \frac{J^2}{4r^2} \quad (3.5)$$

is shifted by $1/(4r^2)$ in order to guarantee the correct behaviour of the WKB solution at the origin. In Eq. (3.4), t is the simple zero of Q^2 .

Given the function Q , it is possible to determine the WKB condition for asymptotic QNMs. The methodology that we adopt has been explained in details in [9]. First, one determines the zeros and poles of the function Q and consequently the behavior of the Stokes and anti-Stokes lines in the complex r -plane. Stokes lines are the lines on which the WKB phase ($\int Q dr$) is purely imaginary and anti-Stokes lines are the lines on which the WKB phase is purely real. It turns out that for Schwarzschild black holes in any spacetime dimension, there are two unbounded anti-Stokes lines which extend to infinity on either side of a bounded anti-Stokes line that encircles the event horizon. In the case of R-N black hole, which has two horizons, the unbounded anti-Stokes lines are again on either side of a bounded anti-Stokes line encircling both the event horizon and the inner Cauchy horizon. Inside this loop a second bounded anti-Stokes line encircles the inner Cauchy horizon. The structure of anti-Stokes lines for Schwarzschild and R-N black holes in four and higher dimensions can be found in [10].

To determine the WKB condition on the QNM frequency we start on an unbounded anti-Stokes line where the solution is known due to the boundary condition at infinity:

$$\psi_{initial} = \Psi_\infty . \quad (3.6)$$

It is relatively simple to determine how the solutions change as we move along an anti-Stokes line. Moreover, there are rules that specify how the solution changes when one moves from one anti-Stokes line to another while crossing Stokes lines. The procedure is to move along a contour that goes from the known solution at infinity along the unbounded anti-Stokes line, changes to the bounded anti-Stokes line(s), loops around the event horizon and finally returns to infinity along the same unbounded anti-Stokes line that it started

from. This yields a final wave solution ψ_{final} that is related to the one we started from as follows:

$$\psi_{final} = \chi \Psi_{initial} , \quad (3.7)$$

where χ is the monodromy of this contour. Since this contour circles only one pole, namely the horizon, the monodromy of this contour must be the same as the monodromy of a contour in the vicinity of the pole at the event horizon. This latter monodromy is determined by the boundary condition at the horizon, so that we are left with a consistency condition that determines asymptotic QNMs.

Applying the above method to Schwarzschild black holes in four and higher dimensions one arrives at the condition

$$e^{2i\Gamma} = -1 - 2 \cos\left(\frac{J}{n}\pi\right) , \quad (3.8)$$

where the appropriate value of J is given in (3.3). Γ is the integral of the function Q along a contour encircling the pole at the event horizon in the negative direction. Using the residue theorem to evaluate Γ yields

$$\Gamma = \oint Q dy = -2\pi i \operatorname{Res}_{r=|r_h|} Q = -2\pi i \left[\frac{1}{n-1} (2\mu)^{1/(n-1)} \omega \right] . \quad (3.9)$$

We can now combine Eqs. (3.3), (3.8), and (3.9) to evaluate ω :

$$\frac{4\pi}{n-1} (2\mu)^{\frac{1}{n-1}} \omega = \ln(3) + (2k+1)\pi i \quad \text{as } k \rightarrow \infty \quad (3.10)$$

This result is valid for all types of metric perturbations in four and higher dimensions.

In the R-N case where $\theta \neq 0$, the same procedure yields the following general WKB condition for four and higher dimensions:

$$e^{2i\Gamma_e} = 1 - 2 \left[1 + \cos\left(\frac{J}{2n-1}\pi\right) \right] (1 + e^{-2i\Gamma_i}) , \quad (3.11)$$

where Γ_e and Γ_i are the integral of the function Q along a contour encircling the pole at the event horizon and the inner Cauchy horizon respectively in the negative direction. We can also evaluate these integrals using the residue theorem, and the results are

$$\Gamma_e = -2\pi i \operatorname{Res}_{r=|r_+|} Q = -\pi i \frac{r_+^n \omega}{(n-1)\sqrt{\mu^2 - \theta^2}} , \quad (3.12)$$

and

$$\Gamma_i = -2\pi i \operatorname{Res}_{r=|r_-|} Q = \pi i \frac{r_-^n \omega}{(n-1)\sqrt{\mu^2 - \theta^2}} . \quad (3.13)$$

Here r_+ and r_- are the locations of the event horizon and the inner Cauchy horizon respectively, which are given by

$$r_{\pm} = \left(\mu \pm \sqrt{\mu^2 - \theta^2} \right)^{\frac{1}{n-1}} . \quad (3.14)$$

Since in this paper we are interested in the Schwarzschild limit of Eq. (3.17), let us find ω in the limit where $\theta \rightarrow 0$, we note that in this limit:

$$\Gamma_e \approx -\frac{2\pi i}{n-1} \omega (2\mu)^{\frac{1}{n-1}}, \quad (3.15)$$

and

$$\Gamma_i \approx \frac{\pi i}{n-1} \omega \mu^{\frac{1}{n-1}} \left(\frac{\theta^2}{2\mu^2} \right)^{\frac{n}{n-1}}. \quad (3.16)$$

Equation (3.11) then takes the simple form

$$\exp\left(\frac{4\pi}{n-1} (2\mu)^{\frac{1}{n-1}} \omega\right) \approx -3 - 4 \cos\left(\frac{J}{2n-1} \pi\right). \quad (3.17)$$

The constant J for tensor and scalar perturbations is $n-1$, while for vector perturbations it is $2n$. Even though J is different in vector perturbations, but for these perturbations we can write

$$\frac{J_{vector}}{2n-1} = \frac{2n}{2n-1} = 2 - \frac{n-1}{2n-1}, \quad (3.18)$$

which produces the same result in Eq. (3.17) as tensor and scalar perturbations for which

$$\frac{J}{2n-1} = \frac{n-1}{2n-1}. \quad (3.19)$$

Thus, in the small charge limit, the R-N black hole QNM frequency is:

$$\frac{4\pi}{n-1} (2\mu)^{\frac{1}{n-1}} \omega \approx \ln\left[3 + 4 \cos\left(\frac{n-1}{2n-1} \pi\right)\right] + (2k+1)\pi i \quad \text{as } k \rightarrow \infty. \quad (3.20)$$

Clearly this does not correspond with the Schwarzschild result in Eq. (3.10). The difference, as pointed out in [9] is due to the order in which the limits $|\omega| \rightarrow \infty$ and $\theta \rightarrow 0$ are taken. This issue will be addressed in detail in the following sections.

Note that the results in this section are consistent with the results obtained by Nataro and Schiappa in [10], where the reader can find a detailed calculation of the highly damped QNMs based on the different methodology first used in [5] and [11].

4. Schwarzschild Limit of Reissner-Nordström Black Holes

It was shown in the previous section that the infinitely damped QNM frequencies of R-N black holes do not approach the Schwarzschild result in the limit when the black hole charge goes to zero. This is a potentially puzzling issue that deserves more careful investigation. The resolution was suggested in [9]: there should be an intermediate regime of large but finite damping in which QNMs resemble the Schwarzschild result. We now investigate this issue using a combination of analytic and numerical methods to carefully track the modification in the structure of the Stokes and anti-Stokes lines in the complex plane as we approach the Schwarzschild limit. We will of necessity concentrate only on vector perturbations because in tensor and scalar perturbations the constant J is zero for Schwarzschild black holes where $\theta = 0$, which makes the numerical analysis problematic

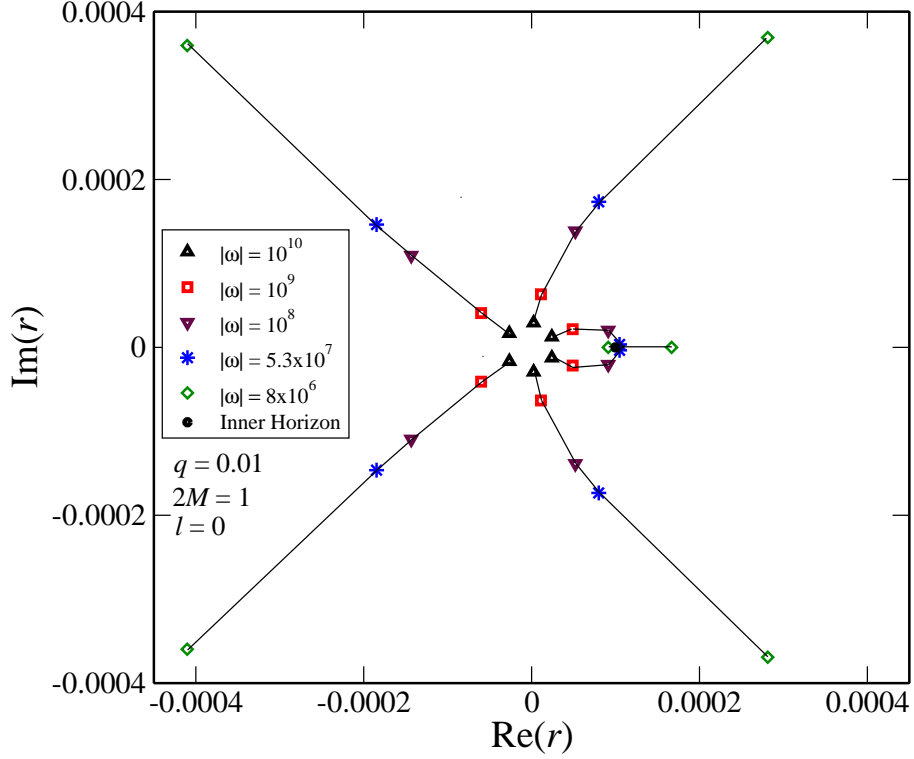


Figure 1: The zeros of the function Q for pure gravitational axial perturbations in four spacetime dimensions for different values of $|\omega|$.

in the Schwarzschild limit. Note that the analytic calculations stay away from $J = 0$ until the end, and then take the limit $J \rightarrow 0$ in the final expression for the frequencies.

In the case of R-N black hole, for vector electromagnetic-gravitational perturbations one has two distinct effective potentials

$$V_{v\pm} = f(r) \left[-\frac{n(n-2)}{4}\lambda + \frac{4l(l+n-1) + n(n-2)}{4r^2} + \frac{\beta_{\pm}\mu}{r^{n+1}} + \frac{n(5n-2)\theta^2}{4r^{2n}} \right], \quad (4.1)$$

where

$$\beta_{\pm} = -\frac{n^2+2}{2} \pm \sqrt{(n^2-1)^2 + 2n(n-1)[l(l+n-1) - n] \frac{\theta^2}{\mu^2}}. \quad (4.2)$$

Setting $\lambda = 0$ we get

$$R_{v\pm}(r) = \frac{1}{f^2} \left\{ \omega^2 - \frac{4l(l+n-1) + n(n-2)}{4r^2} + \frac{4l(l+n-1) + 3n^2 - 4n - \beta_{\pm}\mu}{2r^{n+1}} \mu - \frac{n^2 - 1 - 2\beta_{\pm}\mu^2}{r^{2n}} - \frac{n(7n-5) + \frac{n}{4}(n-2) + l(l+n-1)}{r^{2n}} \theta^2 + \frac{3n(n-1) + \frac{n}{2}(5n-2) - \beta_{\pm}\mu\theta^2}{r^{3n-1}} - \frac{n(n-1) + \frac{n}{4}(5n-2)}{r^{4n-2}} \theta^4 \right\}. \quad (4.3)$$

Since we are interested in the Schwarzschild limit, throughout this paper we take $\theta/\mu \ll 1$, where the coupled electromagnetic and gravitational vector perturbations approach pure

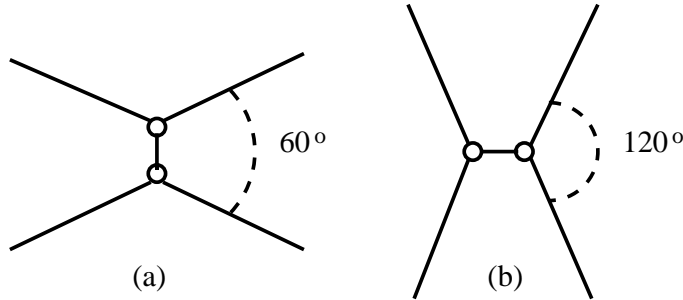


Figure 2: Anti-Stokes lines emanating from the two zeros *before* (a) and *after* (b) they coincide on the real axis.

electromagnetic and gravitational perturbations. In this limit, for electromagnetic waves we have $\beta_+ \approx n^2/2 - 2$ and for gravitational waves we have $\beta_- \approx -3n^2/2$. In order to do numerical analysis, let us concentrate first on four dimensional spacetime where the function R for pure electromagnetic and gravitational perturbations is

$$R(r) \approx \frac{1}{f^2} \left\{ \omega^2 - \frac{l(l+1)}{r^2} + \frac{j^2 + l(l+1)}{r^3} 2M - \frac{j^2 - 1/4}{r^4} (2M)^2 + \frac{j^2 + 6}{r^5} 2Mq^2 - \frac{6}{r^6} q^4 \right\}. \quad (4.4)$$

Here q and M are the charge and mass of the black hole respectively and j is the spin of the perturbation which is 1 for electromagnetic and 2 for gravitational perturbations. Note that in the infinite damping limit, where $-\text{Im } \omega \rightarrow \infty$, the zeros of the function R approach the origin of the complex plane and as in Eq. (3.2) one can always take

$$R(r) \sim \frac{\omega^2}{f^2} - \frac{6}{r^2}. \quad (4.5)$$

On the other hand, for large but finite damping, where $-\text{Im } \omega \gg \text{Re } \omega$, the zeros of the function R are not infinitely close to the origin of the complex plane. In this case we need in principle to consider all the terms in the function R . The terms in Eq. (4.4) of order r^{-3} and r^{-2} inside the curly bracket are in fact negligible as long as the zeros of the function R are located at a radius much smaller than 1, but for the sake of accuracy, we nonetheless keep all the terms in Eq. (4.4) in our numerical calculations.

Fig. 1 shows how the zeros of the function $Q^2 = R - \frac{1}{4r^2}$, for pure gravitational axial perturbations ($j = 2$), move in the complex plane as we change the value of $|\omega|$. (In our calculations we always assume that $|\omega| = |\text{Im } \omega|$.) In this figure we have taken $l = 0$, $2M = 1$, and $q = 0.01$. As $|\omega|$ decreases, four of the zeros move away from the origin and approach the Schwarzschild limit in which the zeros are located at $r_0 \approx |r_0| e^{(2k+1)\pi/4}$, where $k = 0, 1, 2, 3$. The remaining two zeros, located on the right side of the origin, initially move away from the origin and then they move toward the positive real axis, where they eventually coincide at a point to the right of the inner horizon. In Fig. 1, the two zeros coincide when the damping is approximately equal to 5.3×10^7 . After they coalesce, one zero moves toward the inner horizon and the other one moves away from the inner horizon. This motion does not continue indefinitely. In Fig. 1, the two zeros on the real axis asymptote to $r = 0.00009122 \dots$, which is just inside the inner horizon, and

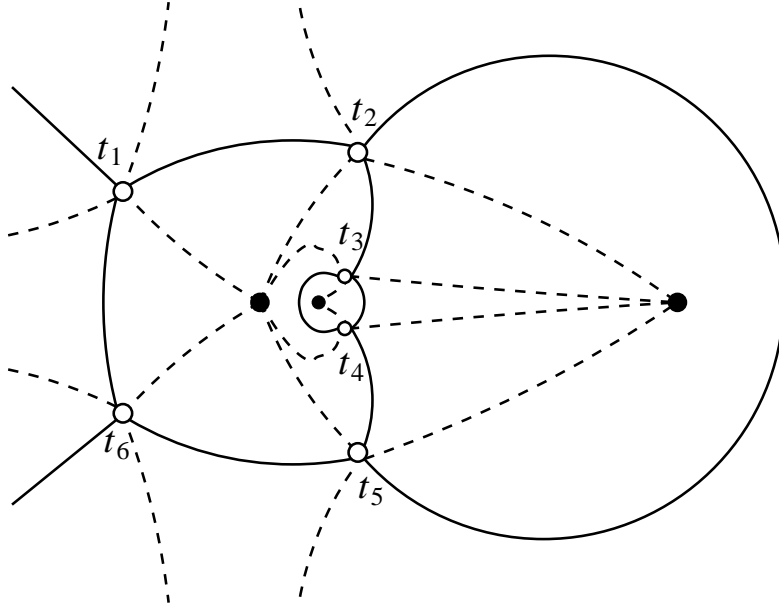


Figure 3: Schematic presentation of Stokes (dashed) and Anti-Stokes (solid) lines in the complex plane *before* the two zeros coincide. The open circles are the zeros and the filled circles are the poles of the function Q^2 .

$r = 0.00017133\dots$, which is just outside the inner horizon. Thus, two of the zeros stay relatively close to the inner horizon while the other zeros move far away from the origin. These four zeros finally enter a region in the complex plane far enough away from the origin so that the terms with the charge q in the functions f , R , and Q become negligible. This happens in the range

$$\frac{(j^2 - 1) + 3/4}{(2M)^2} \ll |\omega|^2 \ll \frac{4(j^2 - 1) + 3}{M^2} \left(\frac{M}{q}\right)^8. \quad (4.6)$$

For $q/M \ll 1$, this nonetheless allows many orders of magnitude for $|\text{Im } \omega|$. In this range, we can approximate Q^2 to be

$$Q^2(r) \sim \frac{1}{f^2} \left\{ \omega^2 - \frac{[(j^2 - 1) + 3/4](2M)^2}{r^4} \right\} - \frac{1}{4r^2}, \quad (4.7)$$

which is exactly identical to what we have for Schwarzschild black holes.

It is important to look carefully at what happens when two of the zeros merge on the real axis. Fig. 2(a), shows the two zeros just before they coincide on the real axis. The two anti-Stokes lines to the left encircle the inner horizon and the two anti-Stokes lines to the right connect to the neighboring zeros on either side of the positive real axis. After the zeros coincide the angle between the anti-Stokes lines on the right hand side, which was 60° before they coincide, has changed to 120° as one can see in Fig. 2. During this transition, the lines must break apart. The anti-Stokes lines to the right detach from their neighboring zeros and encircle the pole at the origin. The schematic behavior of the Stokes and anti-Stokes lines *before* and *after* the two zeros coincide on the real axis are shown in Figs. 3

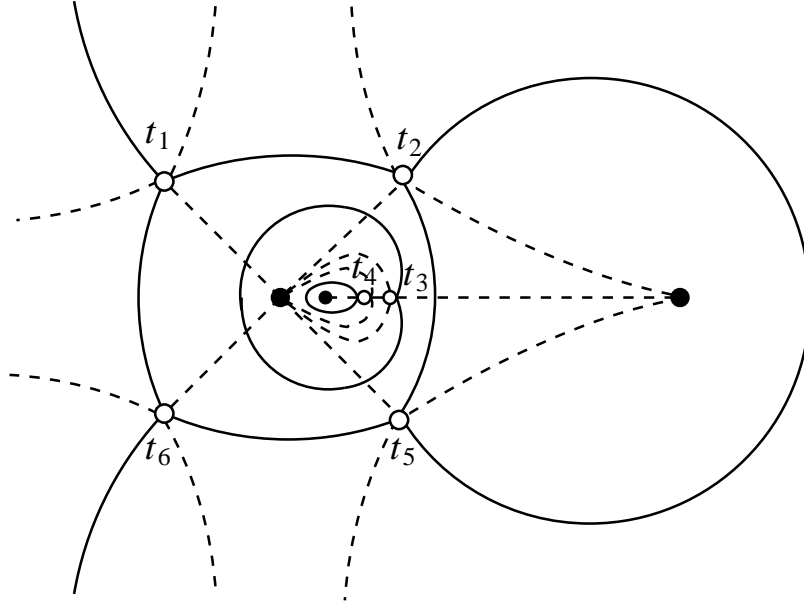


Figure 4: Schematic presentation of Stokes (dashed) and Anti-Stokes (solid) lines in the complex plane *after* the two zeros coincide. The open circles are the zeros and the filled circles are the poles of the function Q^2 .

and 4 respectively. These schematic figures are based on numerically generated diagrams of Stokes and anti-Stokes lines in the complex plane. An example of such numerically generated diagrams is shown in Fig. 5, which plots the Stokes and anti-Stokes lines for the gravitational perturbations ($j = 2$) with $l = 0$, $2M = 1$, $q = 0.01$, and $|\omega| = 5 \times 10^6$. Note that Fig 5 shows that at this point one of the zeros is located inside the inner horizon.

The numerical recipe we have written is operating in the following way: The input parameters are j , M , q , ω , the exact position of the zeros of the function Q , and the approximate angles in which the Stokes and anti-Stokes lines emanate from those zeros. In the program we use the fact that

$$\int_a^{a+dz} \sqrt{Q(r)} dr = \frac{2}{3} \frac{1}{Q'(a)dz} \left[(Q(a) + Q'(a)dz)^{3/2} - Q(a)^{3/2} \right], \quad (4.8)$$

when the stepsize $|dz|$ is small enough. The numerical calculation starts at the zeros of the function Q . To find the Stokes lines, the program finds the point where

$$-\epsilon \leq \text{Re} \left\{ \frac{2}{3} \frac{1}{Q'(a)dz} \left[(Q(a) + Q'(a)dz)^{3/2} - Q(a)^{3/2} \right] \right\} \leq \epsilon, \quad (4.9)$$

and to find the anti-Stokes lines the program finds the points where

$$-\epsilon \leq \text{Im} \left\{ \frac{2}{3} \frac{1}{Q'(a)dz} \left[(Q(a) + Q'(a)dz)^{3/2} - Q(a)^{3/2} \right] \right\} \leq \epsilon. \quad (4.10)$$

Here ϵ ideally needs to be zero but in the numerical calculations we take it to be a small number which generally works well if we take it to be roughly equal to the stepsize $|dz|$.

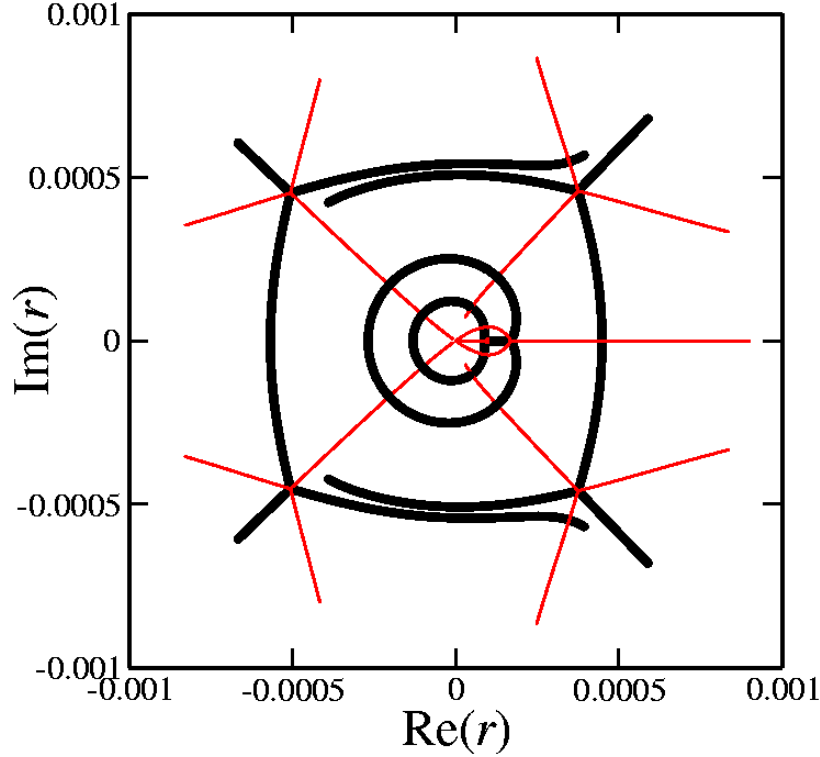


Figure 5: Stokes and anti-Stokes lines produced by numerical calculations for pure gravitational axial perturbations, where $l = 0$, $2M = 1$, and $q = 0.01$.

As the program calculates the direction of the lines and moves away from the zeros the numerical error gets bigger. This is the reason why some times the lines miss each other and they move close to each other until the program cannot find any more points as seen in Fig. 5.

We can use also the numerically generated Stokes and anti-Stokes lines to calculate the QNM frequency. First, we use the method of [9] to find the general WKB condition

$$e^{2i\Gamma} = -e^{2i\gamma_{52}} - \frac{(1 + e^{2i\gamma_{52}})}{e^{2i\gamma_{12}}} \quad (4.11)$$

for the topology shown in Fig. 4. Here

$$\gamma_{ab} = \int_{t_a}^{t_b} Q(r)dr , \quad (4.12)$$

and Γ is given in Eq. (3.9) when $n = 2$. In the Schwarzschild topology, where $\gamma_{12} = \gamma_{52} = -\pi$, Eq. (4.11) reduces to the WKB condition we found in Eq. (3.8) in four spacetime dimensions. The phase integrals γ_{12} and γ_{52} can be calculated numerically. For the particular case in Fig. 5 we find $\gamma_{12} \sim -3.076 \cdots$ radians and $\gamma_{52} \sim -3.447 \cdots$ radians. Therefore we get

$$e^{2i\Gamma} = e^{8\pi\omega M} \approx -2.547 \cdots + i1.380 \cdots . \quad (4.13)$$

In other words $\text{Re } \omega M \approx \ln(2.897 \cdots)/8\pi$.

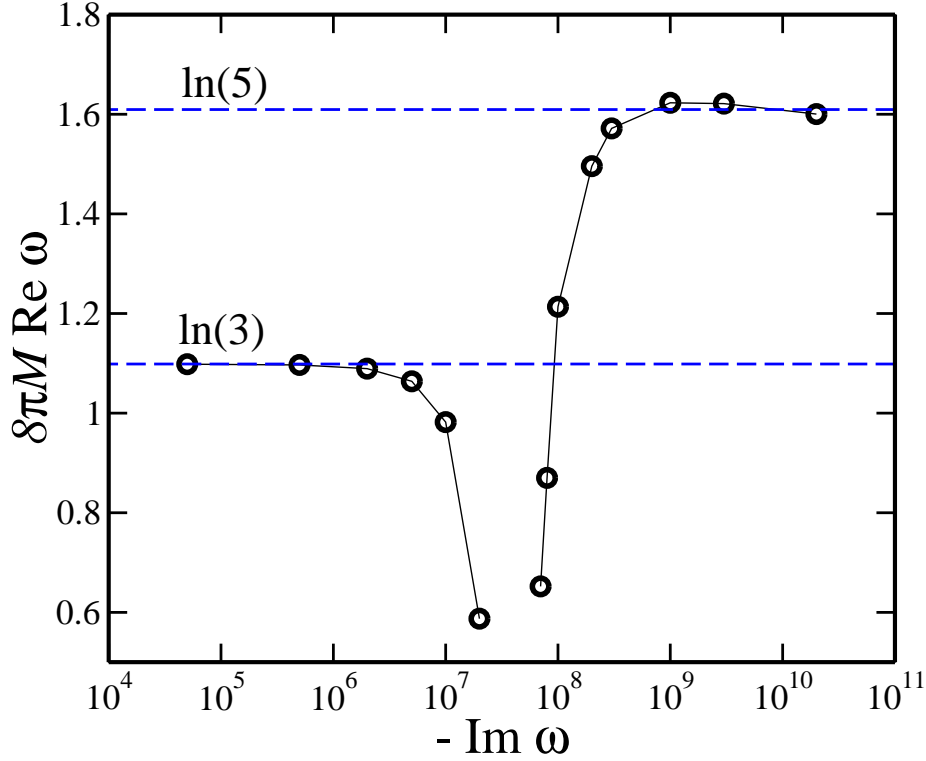


Figure 6: $8\pi M \text{Re } \omega$ as a function of $-\text{Im } \omega$ for pure gravitational axial perturbations, where $l = 0$, $2M = 1$, and $q = 0.01$.

Similar to Eq. (4.11), we can find a general expression for the WKB condition for the topology shown in Fig. 3:

$$e^{2i\Gamma_e} = 1 - (1 + e^{2i\gamma_{12}})(1 + e^{-2i\gamma_{32}})e^{-2i\gamma_{12}}e^{2i\gamma_{32}}(1 + e^{-2i\Gamma_i}e^{2i\tilde{\gamma}_{43}}e^{2i\gamma_{32}}), \quad (4.14)$$

where Γ_e and Γ_i are given in Eqs. (3.12) and (3.13) respectively when $n = 2$. To obtain the WKB condition (4.14), we have used the fact that $\gamma_{32} = \gamma_{54}$ by symmetry. Note that the WKB conditions (4.11) and (4.14) are also valid in higher spacetime dimensions.

In the limit $q/M \ll 1$, we can write

$$\Gamma_e \approx -4\pi i \omega M \left(1 + \frac{q^4}{16M^4}\right) \approx -4\pi i \omega M, \quad (4.15)$$

and

$$\Gamma_i \approx \pi i \omega M \left(\frac{q^4}{4M^4}\right). \quad (4.16)$$

Therefore, Eq. (4.14) can be approximated to be

$$e^{8\pi\omega M} \approx 1 - (1 + e^{2i\gamma_{12}})(1 + e^{-2i\gamma_{32}})e^{-2i\gamma_{12}}e^{2i\gamma_{32}}(1 + e^{2i\gamma_{43}}e^{2i\gamma_{32}}). \quad (4.17)$$

We can now numerically calculate the phase integrals γ_{12} , γ_{32} , and γ_{43} and evaluate the real part of ω by using the WKB condition (4.17).

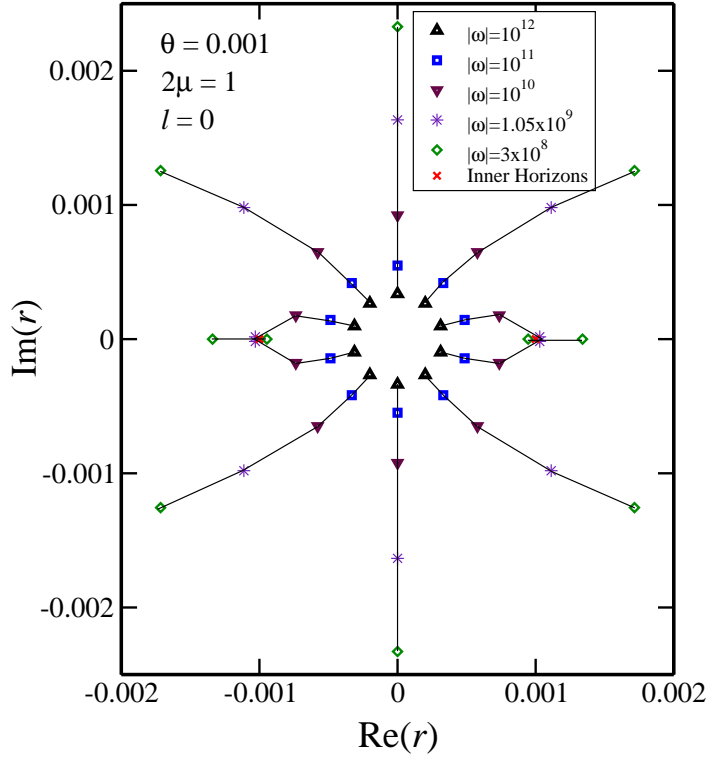


Figure 7: The zeros of the function Q for pure gravitational vector perturbations in 5- d for different values of $|\omega|$.

Fig. 6 plots $8\pi M \text{Re } \omega$ as a function of $-\text{Im } \omega$ for pure gravitational axial perturbations, where we have taken $l = 0$, $2M = 1$, and $q = 0.01$. It is interesting to note that at the point where the topology changes from R-N to Schwarzschild, the real part of the QNM frequency approaches to zero.

5. Schwarzschild Limit in Higher Spacetime Dimensions

So far we have concentrated on the metric perturbations in four spacetime dimensions. The same type of numerical analysis can readily be done in higher spacetime dimensions and one expects similar results. The crucial point is that as the magnitude of the frequency ω changes, there should be a topology change of the kind which is shown in Figs. 3 and 4. This type of topology change happens when two of the zeros of the function Q , which are off the real axis initially, coincide on the real axis and then move along the real axis staying relatively close to the inner Cauchy horizon. We plot the zeros of the function Q for pure gravitational vector perturbations in five spacetime dimensions for different values of $|\omega|$ in Fig. 7 and give the corresponding results for the real part of the QNM frequencies in Fig. 8 respectively.

We expect this behaviour is generic to all dimensions: in $d = n + 2$ dimensions there are, in the R-N case, two times $(n - 1)$ horizons distributed in pairs along equally spaced radial lines in the complex plane. The physical pair is, of course, on the real axis. In the Schwarzschild limit Q^2 has $2n$ zeros, while in the R-N limit it has $4n - 2$. The difference

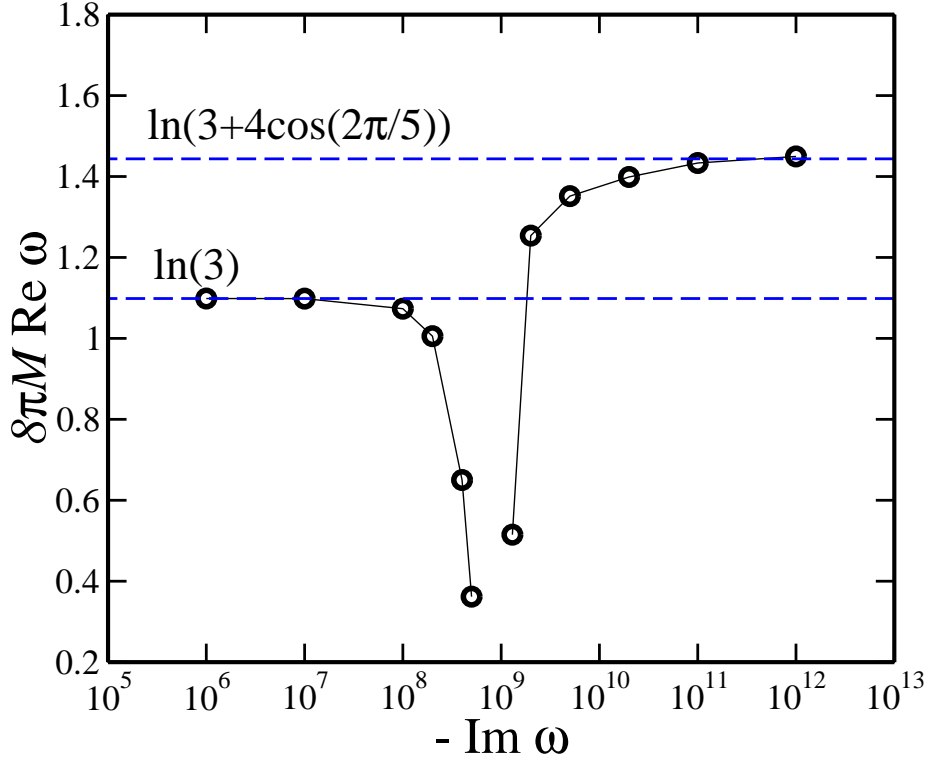


Figure 8: $8\pi\text{Re } \omega M$ as a function of $-\text{Im } \omega$ for pure gravitational vector perturbations in 5- d , where $l = 0$, $2\mu = 1$, and $\theta = 0.001$.

is $2(n-1)$ zeros, which converge in pairs near the $n - 1$ inner horizons and then move apart at right angles. This behaviour should occur in the range:

$$1 \ll |\omega|^2 M^{2/(n-1)} \ll \left(\frac{M}{q}\right)^{4n/(n-1)}. \quad (5.1)$$

There will be a critical value of the damping in this range for which the pairs coincide and the real frequency will be zero or near zero. In Figs. 7 and 8, this critical damping happens at approximately 1.05×10^9 .

6. Conclusions

We have calculated explicitly the QNM frequencies of R-N black holes in the transition region of damping that interpolates between the R-N and Schwarzschild limits. Our numerical results suggest that the real part of the frequency decreases to zero from its $\ln(3)$ Schwarzschild value at a critical value of the damping before increasing to the R-N value. This behaviour is due to the discontinuous nature of the transition from six evenly spaced zeros of the WKB phase to four evenly spaced zeros, with two zeros even closer to the origin. In particular the two zeros first meet near the horizon at the critical value of the damping and then emerge at right angles. It is at this stage that the Stokes lines undergo a discrete topology change and the real part of the frequency goes to zero. We

have shown that this behaviour is also present in five dimensions, and argued that it is a generic feature of all higher dimensional R-N black holes.

The physical interpretation of the highly damped QNM frequencies in terms of the quantum spectrum of black holes is highly speculative, and seems to be contradicted by a myriad of results for multi-horizon, non-asymptotically flat black holes. It should be noted, however, that Hod's original conjectures only apply directly to single horizon black holes, whose horizons are described by one dimensionful parameter, which could without loss of generality be taken as the temperature. The present analysis, in our opinion, seems to reverse slightly this negative trend. In effect, we have shown explicitly that for R-N black holes with small charge, the infinitely damped QNMs essentially "see" the full structure of the solution, including the inner horizon, which affects the value of the frequency in this limit. There is nonetheless an intermediate damping for which the QNMs only probe the outer horizon, and for this range the "universal" value of $\ln(3)$ is reproduced.

It therefore seems that this issue is worthy of continued investigation.

Acknowledgments

This research was supported in part by the Natural Sciences and Engineering Research Council of Canada.

References

- [1] S. Hod, *Phys. Rev. Lett.* **81** (1998) 4293.
- [2] O. Dreyer, *Phys. Rev. Lett.* **90** (2003) 081301.
- [3] J.D. Bekenstein, *Lett. Nuovo. Cim.* **4** (1972) 737.
- [4] G. Kunstatter, *Phys. Rev. Lett.* **90** (2003) 161301; V. Cardoso and J. P. S. Lemos, *Phys. Rev.* **D67** (2003) 084020; S. Hod, *Phys. Rev.* **D67** (2003) 081501; E. Abdalla, K. H. C. Castello-Branco and A. Lima-Santos, *Mod. Phys. Lett.* **A18** (2003) 1435; E. Berti and K. D. Kokkotas, *Phys. Rev.* **D68** (2003) 044027; H. T. Cho, *Phys. Rev.* **D68** (2003) 024003; A. Maassen van den Brink, *J. Math. Phys.* **45** (2004) 327; K. Glampedakis and N. Andersson, *Class. Quant. Grav.* **20** (2003) 3441; C. Molina, *Phys. Rev.* **D68** (2003) 064007; A. P. Polychronakos, *Phys. Rev.* **D69** (2004) 044010; A. Maassen van den Brink, *Phys. Rev.* **D68** (2003) 047501; L. H. Xue, Z. X. Shen, B. Wang and R. K. Su, *Mod. Phys. Lett.* **A19** (2004) 239; V. Cardoso, R. Konoplya and J. P. S. Lemos, *Phys. Rev.* **D68** (2003) 044024; D. Birmingham, S. Carlip and Y. j. Chen, *Class. Quant. Grav.* **20** (2003) L239; D. Birmingham, *Phys. Lett.* **B569** (2003) 199; E. Berti and K. D. Kokkotas, *Phys. Rev.* **D67** (2003) 064020; E. Berti, V. Cardoso, K. D. Kokkotas and H. Onozawa, *Phys. Rev.* **D68** (2003) 124018; E. Berti, V. Cardoso and S. Yoshida, *Phys. Rev.* **D69** (2004) 124018; J. Oppenheim, *Phys. Rev.* **D69** (2004) 044012; S. Yoshida and T. Futamase, *Phys. Rev.* **D69** (2004) 064025; S. Musiri and G. Siopsis, *Class. Quant. Grav.* **20** (2003) L285; S. Musiri and G. Siopsis, *Phys. Lett.* **B579** (2004) 25; R. A. Konoplya, *Phys. Rev.* **D68** (2003) 124017; R. Konoplya, *Phys. Rev.* **D71** (2005) 024038; V. Cardoso, J. P. S. Lemos and S. Yoshida, *Phys. Rev.* **D69** (2004) 044004; A. J. M. Medved, D. Martin and M. Visser, *Class. Quant. Grav.* **21** (2004) 1393; A. J. M. Medved, D. Martin and M. Visser, *Class. Quant. Grav.* **21**

- (2004) 2393; T. R. Choudhury and T. Padmanabhan, *Phys. Rev. D* **69** (2004) 064033; M. R. Setare, *Class. Quant. Grav.* **21** (2004) 1453; M. R. Setare, *Phys. Rev. D* **69** (2004) 044016; V. Cardoso, J. P. S. Lemos and S. Yoshida, *JHEP* **0312** (2003) 041; H. b. Zhang, Z. j. Cao, X. f. Gong and W. Zhou, *Class. Quant. Grav.* **21** (2004) 917; J. l. Jing, *Phys. Rev. D* **69** (2004) 084009; L. Vanzo and S. Zerbini, *Phys. Rev. D* **70** (2004) 044030; T. Tamaki and H. Nomura, *Phys. Rev. D* **70** (2004) 044041; V. Cardoso, J. Natario and R. Schiappa, *J. Math. Phys.* **45** (2004) 4698; D. P. Du, B. Wang and R. K. Su, *Phys. Rev. D* **70** (2004) 064024; C. Kiefer, *Class. Quant. Grav.* **21** (2004) L123; A. Ohashi and M. a. Sakagami, *Class. Quant. Grav.* **21** (2004) 3973; E. Berti, V. Cardoso and J. P. S. Lemos, *Phys. Rev. D* **70** (2004) 124006; S. b. Chen and J. l. Jing, *Class. Quant. Grav.* **22** (2005) 533; S. Lepe and J. Saavedra, *Phys. Lett. B* **617** (2005) 174; F. W. Shu and Y. G. Shen, *Phys. Rev. D* **70** (2004) 084046; K. H. C. Castello-Branco, R. A. Konoplya and A. Zhidenko, *Phys. Rev. D* **71** (2005) 047502; S. Fernando and C. Holbrook, hep-th/0501138; F. W. Shu and Y. G. Shen, *Phys. Lett. B* **619** (2005) 340; J. l. Jing and Q. y. Pan, *Phys. Rev. D* **71** (2005) 124011; J. l. Jing, *Phys. Rev. D* **71** (2005) 124006; J. l. Jing, gr-qc/0502010; M. Giammatteo and I. G. Moss, *Class. Quant. Grav.* **22** (2005) 1803; E. Berti and K. D. Kokkotas, *Phys. Rev. D* **71** (2005) 124008; J. f. Chang and Y. g. Shen, *Nucl. Phys. B* **712** (2005) 347; S. b. Chen and J. l. Jing, *Class. Quant. Grav.* **22** (2005) 1129. R. Daghigh and G. Kunstatter, gr-qc/0507019.
- [5] L. Motl and A. Neitzke, *Adv. Theoret. Math. Phys.* **7** (2003) 307.
- [6] J. Kettner, G. Kunstatter, A.J.M. Medved, *Class. Quant. Grav.* **21** (2004) 5317.
- [7] S. Das and S. Shankaranarayanan, *Class. Quant. Grav.* **22** (2005) L7.
- [8] R. Daghigh and G. Kunstatter, *Class. Quant. Grav.* **22** (2005) 4113.
- [9] N. Andersson and C. J. Howls, *Class. Quant. Grav.* **21** (2004) 1623.
- [10] J. Natario and R. Schiappa, hep-th/0411267.
- [11] L. Motl, *Adv. Theoret. Math. Phys.* **6** (2003) 1135.
- [12] E. Berti, "Black hole quasinormal modes: hints of quantum gravity?", gr-qc/0411025.
- [13] A. Ishibashi and H. Kodama, *Prog. Theoret. Phys.* **110** (2003) 701.
- [14] A. Ishibashi and H. Kodama, *Prog. Theoret. Phys.* **110** (2003) 901.
- [15] A. Ishibashi and H. Kodama, *Prog. Theoret. Phys.* **111** (2004) 29.
- [16] G. Gibbons and S. Hartnoll, *Phys. Rev. D* **67** (2002) 064024.
- [17] R. A. Konoplya, *Phys. Rev. D* **68** (2003) 024018.